Reduced 3,4-Methylenedioxymethamphetamine (MDMA, Ecstasy)-Initiated Oxidative DNA Damage and Neurodegeneration in Prostaglandin H Synthase-1 Knockout Mice

Winnie Jeng[†] and Peter G. Wells*[,†,‡,§]

[†]Faculty of Pharmacy and [‡]Department of Pharmacology and Toxicology, University of Toronto, Toronto, Ontario, Canada

Abstract

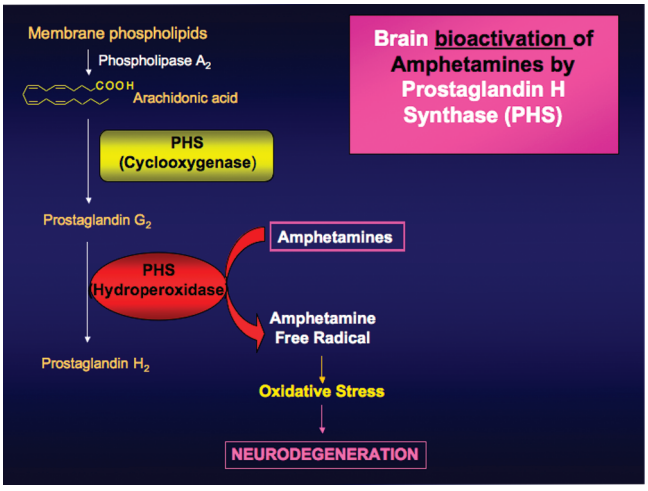

The neurodegenerative potential of 3,4-methylenedioxymethamphetamine (MDMA, ecstasy) and underlying mechanisms are under debate. Here, we show that MDMA is a substrate for CNS prostaglandin H synthase (PHS)-catalyzed bioactivation to a free radical intermediate that causes reactive oxygen species (ROS) formation and neurodegenerative oxidative DNA damage. *In vitro* PHS-1-catalyzed bioactivation of MDMA stereoselectively produced free radical intermediate formation and oxidative DNA damage that was blocked by the PHS inhibitor eicosatetraynoic acid. *In vivo*, MDMA stereoselectively caused gender-independent DNA oxidation and dopaminergic nerve terminal degeneration in several brain regions, dependent on regional PHS-1 levels. Conversely, MDMA-initiated striatal DNA oxidation, nerve terminal degeneration, and motor coordination deficits were reduced in PHS-1 +/− and −/− knockout mice in a gene dose-dependent fashion. These results confirm the neurodegenerative potential of MDMA and provide the first direct evidence for a novel molecular mechanism involving PHS-catalyzed formation of a neurotoxic MDMA free radical intermediate.

Keywords: Ecstasy, 3,4-methylenedioxymethamphetamine, neurodegeneration, prostaglandin H synthase, reactive oxygen species, oxidative DNA damage

3,4-Methylenedioxymethamphetamine (MDMA) is a widely used synthetic amphetamine derivative commonly known as ecstasy. The popularity of MDMA is due to its production of a subtle altered state of consciousness by heightening sensory perception and euphoria, increased energy, and heightened self-acceptance and empathy (*1*). However, problems encountered with MDMA include long-term consequences such as decreased immune function, hepatotoxicity, and kidney failure (*2*, *3*). MDMA has been associated with long-term psychiatric and cognitive effects (*4*−*6*), possibly due to the irreversible loss of monoaminergic nerve terminals and depletion of monoaminergic uptake sites (*7*−*9*). The acute pharmacological effects of MDMA are due to transient, receptor-mediated interactions, which while potentially serious are unlikely to account for the neurodegenerative effects that appear to persist long after drug use (*10*). To add to the mechanistic complexity of neurodegeneration, the long-term effects of MDMA are species- and dose-dependent. In rats and nonhuman primates (*11*, *12*), MDMA and its major metabolite 3,4-methylenedioxamphetamine (MDA) selectively damage serotonergic neurons; however, at larger doses or more frequent exposures, dopaminergic neurons are also affected. In mice, MDMA appears to selectively damage only dopaminergic neurons, apparently without affecting the serotonergic system (*13*). The molecular basis of MDMA neurodegeneration is not well understood.

Cumulative evidence suggests that MDMA and its related amphetamine analogues, methamphetamine (METH) and 3,4-methylenedioxyamphetamine (MDA), are potent and selective neurotoxins that cause monoaminergic neuronal damage through the generation of reactive oxygen species (ROS) (*7*, *14*). In the absence of adequate cytoprotection or repair, ROS can damage cellular macromolecules resulting in altered cellular function and death. A leading hypothesis for the generation of ROS by MDMA and other amphetamines involves their metabolism by cytochromes P450 (CYP) in the brain to the catechol intermediate, 3,4-dihydroxymethamphetamine (*15*).

Received Date: September 30, 2009
Accepted Date: January 12, 2010
Published on Web Date: February 23, 2010

DOI: 10.1021/cn900022w | *ACS Chem. Neurosci.* (2010), *1*, 366–380

This catechol is converted to a reactive quinone that undergoes redox cycling and generates ROS. A more recent variant of this hypothesis involves hepatic metabolism of MDMA to 3,4-dihydroxymethamphetamine (HHMA), catalyzed by CYP2D6 (humans) or CYP2D1 (rats), followed by the formation of a glutathione (GSH)−HHMA conjugate that is transported to the brain, causing neurotoxicity via redox cycling (*16*, *17*). Although there is evidence for CYP-catalyzed metabolism of MDMA, its role in amphetamine neurotoxicity is questionable because of the low concentrations of CYP isoforms in the brain (*18*) and particularly the CYP2D6 isoform that catalyzes the demethylenation of MDMA (*19*). One limiting factor with the HHMA−GSH hypothesis is the direct inhibition of CYP2D6 and CYP2D1 by MDMA (*20*), which limits the peripheral formation of HHMA available for GSH conjugation. Furthermore, the expression of CYP2D6, unlike other CYPs, is resistant to induction by xenobiotics in the liver (*21*) and limited in the brain (*22*). Finally, rats deficient in CYP2D1, the homologue of human CYP2D6, are still susceptible to the neurotoxic effects of MDMA (*23*). Accordingly, if amphetamine neurotoxicity is mediated by ROS, the above discrepancies suggest that other mechanisms or enzymes may contribute to ROS generation by MDMA and related amphetamines.

In a related model with low CYP expression, the developing mouse embryo, our laboratory has found that embryonic prostaglandin H synthase (PHS) can bioactivate xenobiotics to free radical reactive intermediates that initiate the formation of ROS and oxidative macromolecular damage, resulting in teratogenesis (*24*−*27*), and a similar PHS-dependent mechanism in the brain may play a role in the neurodegenerative effects of MDMA (Abstract graphic Figure S1 (Supporting Information)). Herein, we report first an *in vitro* study showing that MDMA is stereoselectively bioactivated by purified PHS to a reactive free radical intermediate that oxidatively damages DNA, which is blocked by the PHS inhibitor eicosatetraynoic acid (ETYA). In a complementary *in vivo* study, PHS-1 knockout mice were protected from the stereoselective neurotoxic effects of MDMA, including DNA oxidation, dopaminergic nerve terminal degeneration, and motor function deficits. The results provide the first direct evidence that PHS-catalyzed bioactivation of MDMA to a free radical intermediate in the brain initiates the formation of ROS that oxidatively damage dopaminergic neurons, resulting in long-lasting functional deficits.

Results

In Vitro Bioactivation of MDMA to Free Radical Reactive Intermediates by PHS-1

PHS-1-catalyzed formation of free radical spin adducts was detected for *dl*-MDMA. (Figure 1, left panel). The EPR signal for *dl*-MDMA after a 1 min incubation revealed a carbon-centered free radical, seen as a triplet of doublets known for this radical adduct (*28*). The triplet of doublets observed for this radical adduct of *dl*-MDMA had hyperfine splitting constants (HFSCs) of a^N = 15.23 G and a_β^H = 3.19 G. The positive control, phenytoin, also gave rise to a carbon-centered free radical with similar HFSCs, a^N = 15.46 G and a_β^H = 2.73 G, that are consistent with previously published observations (Figure 1, left panel) (*29*). The negative control incubation that contained the vehicle solution without MDMA did not show the presence of any radical.

Time-dependent incubation of *dl*-MDMA with PHS-1 that included a longer period of incubation for 5 and 10 min showed a transition from a carbon-centered radical to a nitrogen-centered radical (Figure 1, right panel). Specifically, the 5 and 10 min incubations showed superimposed spectra for both carbon-centered and nitrogen-centered MDMA radicals, the latter of which is characterized by a triplet of sextuplets (*28*).

In Vitro PHS-1-Dependent Oxidation of 2′-Deoxyguanosine (2′-dG) to 8-Oxo-2′-deoxyguanosine (8-oxo-dG) by MDMA

Using the reaction conditions as cited above for the characterization of free radical formation, *dl*-MDMA was bioactivated by PHS-1 *in vitro* to a free radical reactive intermediate that initiated the oxidation of 2′-dG to 8-oxo-dG (Figure 2). Compared to vehicle controls at the lowest amphetamine concentration (0.50 mM), *dl*-MDMA caused a maximal 2.6-fold increase in DNA oxidation ($p < 0.02$) (Figure 2, upper panel). Increasing the *dl*-MDMA concentration to 1 mM did not further increase 2′-dG oxidation, but a significant 1.5-fold increase was maintained ($p < 0.009$). Extending the incubation time from 1 to 10 min with 1 mM *dl*-MDMA resulted in a further increase in the level of 2′-dG oxidation to 2.4-fold ($p < 0.009$) (Figure 2, lower panel). The positive control, phenytoin (0.25 and 0.50 mM), caused a concentration-dependent increase in 2′-dG oxidation from 3.4-fold to 5.1-fold ($p < 0.02$ and $p < 0.006$, respectively) (Figure 2, upper panel), consistent with previously published observations (*29*).

Preincubation of the dual PHS/lipoxygenase inhibitor ETYA (40 μM) with PHS-1 blocked the formation of 8-oxo-dG initiated by 1 mM *dl*-MDMA ($p < 0.001$) (Figure 3). The level of MDMA-initiated DNA oxidation was not decreased in the control incubation containing MDMA with only DMSO, the vehicle for ETYA, confirming that the abolishment of MDMA-initiated DNA oxidation by ETYA was due to the direct inhibition of PHS.

We determined whether stereoselective differences in PHS-dependent DNA oxidation could contribute to the contrasting relative toxicological potencies of the two MDMA enantiomers reported *in vivo*. Co-incubation of

DOI: 10.1021/cn900022w | ACS Chem. Neurosci. (2010), 1, 366–380

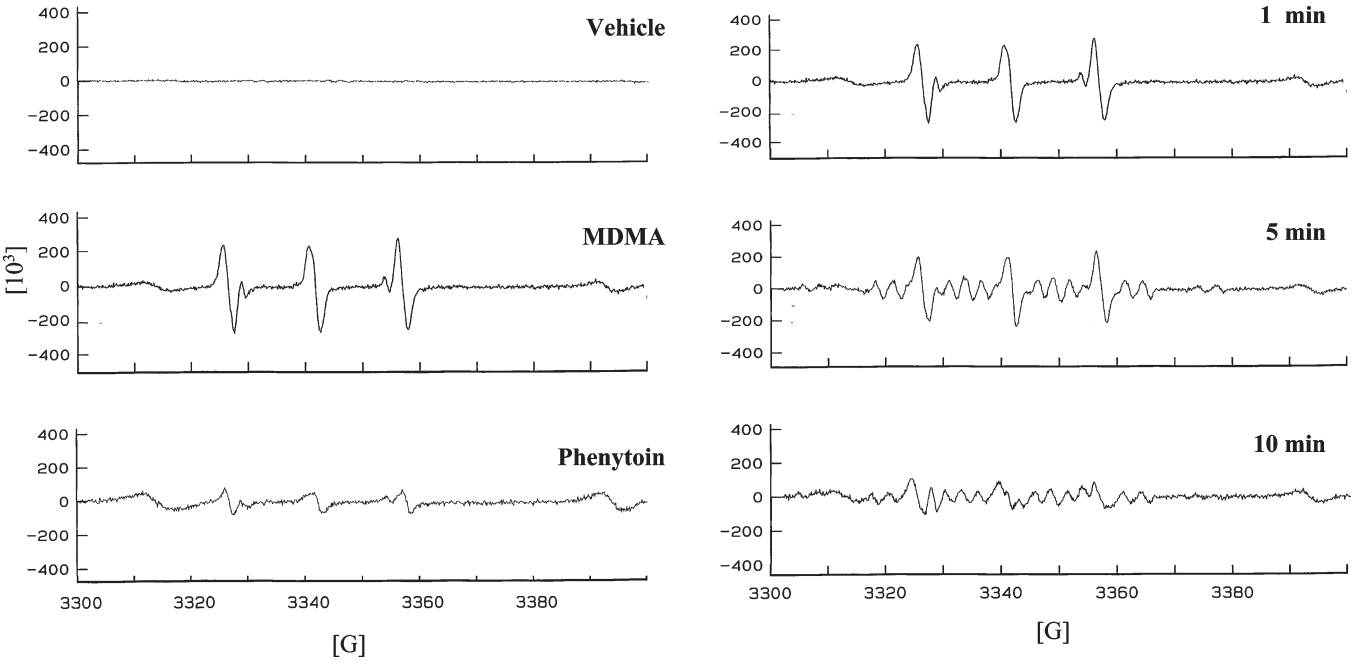

Figure 1. Electron paramagnetic resonance (EPR) spectra for *in vitro* PHS-1-catalyzed bioactivation of amphetamines to free radical intermediates. Left panel: vehicle control (upper panel), 3,4-methylenedioxymethamphetamine (*dl*-MDMA) (middle panel), and phenytoin (lower panel). Each reaction contained 1000U/mL PHS-1, 1.0 μM hematin, and 0.5 mM phenol. After preincubation for 1 min at 37 °C, 67 μM arachidonic acid, 1 mM PBN, and 1 mM of *dl*-MDMA were incubated for 1 min. The positive control phenytoin (0.5 mM) was incubated with PHS for 30 min as previously described (*29*). The vehicle control incubation contained all components except the drug. Right panel: time course for *in vitro* PHS-1-dependent MDMA free radical formation. Shown are the EPR spectra for the incubation of *dl*-MDMA for 1, 5, and 10 min with PHS-1.

d-MDMA (0.5 mM and 1.0 mM) with PHS-1 caused a concentration-dependent increase in oxidative DNA damage which was substantially greater than that caused by its *l*-isomer, with, respectively, 2.3-fold and 4.4-fold increases in DNA oxidation compared to that of the same concentration of *l*-MDMA ($p < 0.04$ and $p < 0.001$, respectively) (Figure 4, upper panel). Compared to the vehicle control, *d*-MDMA at concentrations of 0.5 and 1.0 mM caused, respectively, 7.9-fold ($p < 0.001$) and 56-fold ($p < 0.001$) increases in oxidative DNA damage.

PHS-1-Normal and Knockout Mice *in Vivo*: PHS-Dependent, MDMA-Initiated Regional Increases in Brain DNA Oxidation

In PHS-1-normal +/+ mice, both *dl*-MDMA and *d*-MDMA produced regionally dependent increases in brain DNA oxidation compared to that of their vehicle controls (Figure 4, lower panel). DNA oxidation was measured at 1 h, which previous studies with MDA and METH had determined as the time of maximal oxidative damage initiated in most brain regions by amphetamines (*30*). There were no gender differences in the levels of MDMA-initiated DNA oxidation (data not shown); therefore, DNA oxidation herein represents the combination of female and male values. Within 1 h, *dl*-MDMA ($p < 0.04$) and *d*-MDMA ($p < 0.002$) caused, respectively, 2.8- and 2.4-fold elevations in DNA oxidation in the striatum of +/+ PHS-normal mice, whereas the nontoxic *l*-MDMA isomer was comparable to saline. In contrast, the striatal level of DNA oxidation initiated by *dl*- and *d*-MDMA in the +/+ PHS-1-normal mice was reduced 45% and 33%, respectively, in +/− PHS-deficient mice ($p = 0.057$, $p = 0.06$), and more so, 57% and 46%, respectively, in −/− PHS-deficient mice ($p < 0.05$, $p < 0.009$). A similar gene dose-dependent pattern was seen in the brainstem and substantia nigra, except that the latter was sensitive to *d*-MDMA for all genotypes ($p < 0.05$), suggesting increased susceptibility, possibly due to constitutive PHS-2 expression in that region. DNA oxidation was not enhanced in the cerebellum, cortex, or hippocampus (data not shown), although the latter two regions may exhibit delayed oxidative damage (*30*).

Baseline (constitutive) levels of DNA oxidation in saline-treated mice varied up to 2.0-fold among the brain regions, with the lowest values in the brainstem and cerebellum, and the highest in the hippocampus, striatum, and substantia nigra (Figure 5, upper panel). The constitutive levels depicted in Figure 5 represent the combination of +/+, +/−, and −/− values since there were no differences in baseline levels of DNA oxidation within brain regions among PHS-1 genotypes. DNA oxidation was enhanced up to 6.8-fold among the brain

DOI: 10.1021/cn900022w | *ACS Chem. Neurosci.* (2010), *1*, 366–380

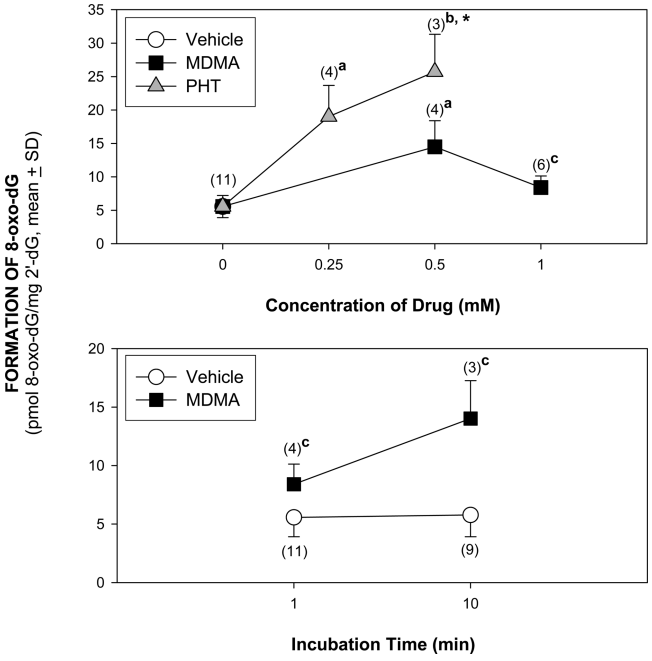

Figure 2. *In vitro* PHS-1-dependent oxidation of DNA initiated by MDMA. Incubations (the number is indicated in parentheses) included 2′-deoxyguanosine (2′-dG), *dl*-MDMA or vehicle, PHS-1, hematin, and arachidonic acid as described in Figure 1 (excluding PBN). Phenytoin (PHT) was the positive control. Oxidative DNA damage was quantified by the formation of 8-oxo-2′-deoxyguanosine (8-oxo-dG). Upper panel: effect of drug concentration at 1 min. $^{a}p < 0.02$, $^{b}p < 0.006$, and $^{c}p < 0.009$ compared to their vehicle control. $*p < 0.02$ compared to 0.25 mM PHT. Lower panel: effect of incubation time. $^{c}p < 0.009$ compared to the vehicle control at the same incubation time point.

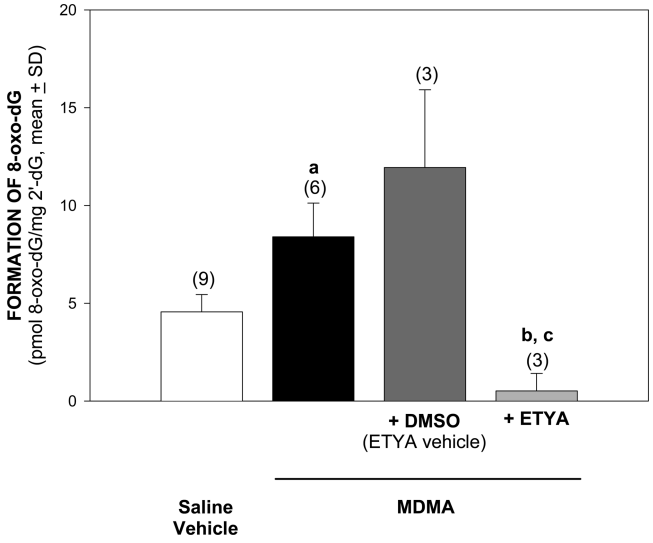

Figure 3. *In vitro* PHS-1-dependent oxidation of MDMA is inhibited by the PHS inhibitor 5,8,11,14-eicosatetraynoic acid (ETYA). Preincubation of the PHS/lipoxygenase inhibitor ETYA (40 μM) with PHS-1 abolished 8-oxo-dG formation for 1 mM *dl*-MDMA. Incubations (the number is indicated in parentheses) included 2′-dG, *dl*-MDMA or its saline vehicle, PHS-1, hematin, and arachidonic acid as described in Figure 1 (excluding PBN). One control incubation included DMSO, the vehicle for ETYA, containing all of the components excluding ETYA. $^{a}p < 0.001$ compared to the saline vehicle, $^{b}p < 0.001$ compared to MDMA, $^{c}p < 0.008$ compared to the DMSO vehicle for ETYA.

regions after *dl*-MDMA treatment, with the highest elevations in the striatum and substantia nigra compared to the lowest level of DNA oxidation in the cerebellum (Figure 5, upper panel). A linear regression analysis showed a positive correlation between baseline DNA oxidation and maximal *dl*-MDMA-enhanced oxidation among the different brain regions from the PHS-1 +/+ mice, which was the only PHS-1 genotype exhibiting a significant increase in oxidative DNA damage ($r = 0.7639$, $p < 0.0022$) (Figure 5, lower panel). This suggests that the constitutive regional level of PHS determines the bioactivation of both endogenous and xenobiotic substrates to DNA-damaging free radical intermediates. The similar levels of endogenous DNA oxidation for a given region among the +/+, +/−, and −/− PHS-1 genotypes suggests a potential contribution to endogenous DNA oxidation from the PHS-2 isozyme.

DNA oxidation was enhanced up to 5.1-fold among the brain regions after *d*-MDMA treatment, with the highest elevations in the striatum and substantia nigra compared to those of the cerebellum. A similar positive correlation was also seen for *d*-MDMA ($r = 0.8482$, $p < 0.0006$) (data not shown).

Endogenous Oxidative DNA Damage in Different Brain Regions Correlates with the Regional Level of PHS

Western blotting revealed substantially different levels of constitutive PHS-1 expression in different regions of the brain, including the cortex, hippocampus, striatum, substantia nigra, brainstem, and cerebellum (Figure S2, Supporting Information). The highest constitutive levels were seen in the substantia nigra and the lowest levels in the cerebellum of PHS-1 +/+ and +/− mice, with a 2.4-fold difference between these brain regions ($p < 0.001$ and $p < 0.001$). PHS-1 protein levels in +/− PHS-1-deficient mice were approximately 50% of those in the +/+ PHS-1-normal mice. Remarkably, a linear regression showed that among the different brain regions, an increasing level of PHS-1 protein correlated positively with increased constitutive DNA oxidation when both copies of the PHS-1 genes are expressed ($r = 0.822$, $p < 0.05$), although the curve for +/− mice was shifted to the left ($r = 0.733$, $p = 0.09$) (Figure S3, Supporting Information).

Stereoselective MDMA-Initiated Ultrastructural Damage to Dopaminergic Nerve Terminals: Protection in −/− PHS-1 Knockout Mice

Striatal degeneration of dopaminergic nerve terminals was seen 1 wk after *d*-MDMA administration (Figure 6, upper panel). Similar to DNA oxidation,

DOI: 10.1021/cn900022w | *ACS Chem. Neurosci.* (2010), *1*, 366–380

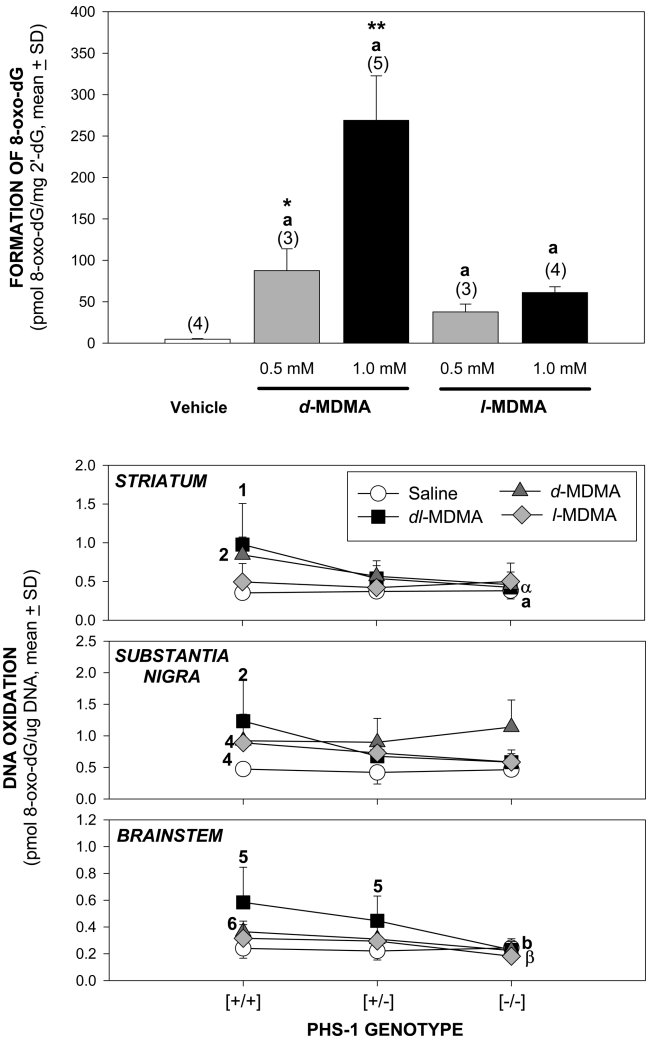

Figure 4. Stereoselectivity in the PHS-1-dependent oxidation of DNA by MDMA enantiomers. Upper panel: *in vitro* PHS-1 oxidation of DNA by MDMA. *d*-MDMA or *l*-MDMA (1 mM) was incubated for 1 min with the components of the *in vitro* system as detailed in Figure 1 (excluding PBN) and analyzed for DNA oxidation. The number of incubations is indicated in parentheses. $^{a}p < 0.001$ compared to the vehicle control; $^{*}p < 0.04$ and $^{**}p < 0.001$ compared to the *l*-enantiomer at the same concentration. Lower panel: PHS-1 knockout mice are protected against brain region-dependent *in vivo* oxidation of DNA by MDMA. *dl*-, *d*-, or *l*-MDMA were dissolved in 0.9% saline and administered in 4 doses (10 mg/kg ip) with each dose given at 2 h intervals. Saline was used as the control. The mice were sacrificed 1 h after the last injection, and tissues from different brain regions were isolated by microdissection and analyzed for oxidative DNA damage. A minimum of 6 mice were used for each group. $^{1,3}p < 0.04$, $^{2}p < 0.002$, $^{4}p < 0.05$, $^{5}p < 0.03$, and $^{6}p < 0.03$ compared to the corresponding saline-treated control for the same PHS-1 genotype. $^{a}p < 0.05$ and $^{b}p < 0.02$ compared to *dl*-MDMA-treated +/+ PHS-1-normal mice. $^{\alpha}p < 0.009$ and $^{\beta}p < 0.006$ compared to *d*-MDMA-treated +/+ PHS-1-normal mice. Note the different scales for levels of DNA oxidation in different brain regions.

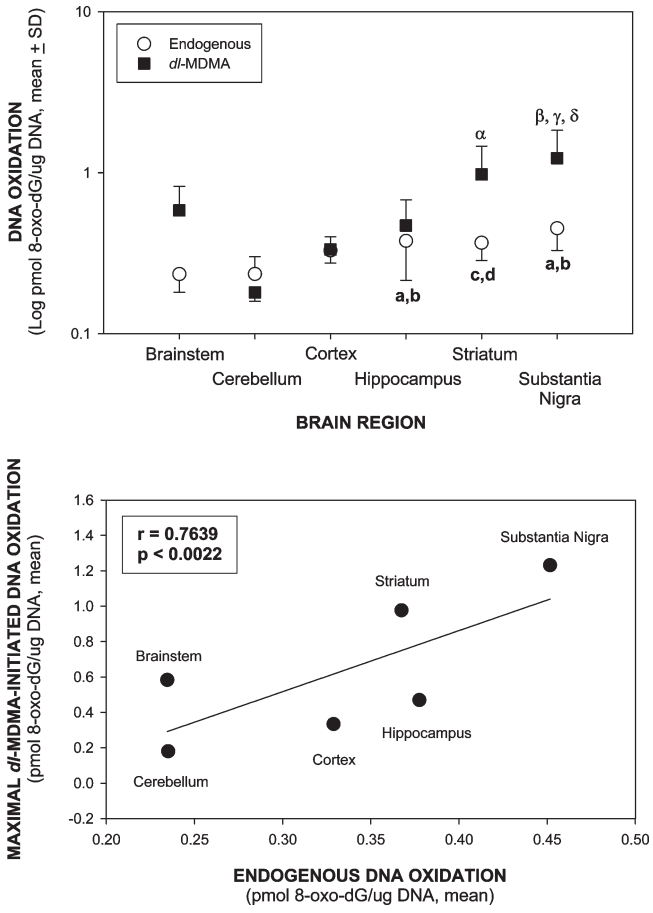

Figure 5. Relationship of baseline (constitutive or endogenous) and MDMA-enhanced DNA oxidation in brain regions of PHS-1 mice. Treatment and analysis of DNA oxidation is as described in Figure 4, lower panel. The constitutive levels represent the combined values for PHS-1 +/+, +/−, and −/− mice, which were identical for a given region. *dl*-MDMA-enhanced DNA oxidation was analyzed only in the PHS-1 +/+ mice, which was the only PHS-1 genotype exhibiting a significant increase in oxidative DNA damage. Upper panel: constitutive and *dl*-MDMA-enhanced DNA oxidation in different brain regions in PHS-1 mice. Lower panel: linear regression curve for constitutive and maximal *dl*-MDMA-initiated DNA oxidation ($R = 0.7639$, $p < 0.0022$). $^{a}p < 0.001$ and $^{c}p < 0.001$ compared to the brainstem and $^{b}p < 0.001$ and $^{d}p < 0.001$ compared to the cerebellum of constitutive brain regions. $^{\alpha}p < 0.05$ and $^{\beta}p < 0.001$ compared to the cerebellum, $^{\gamma}p < 0.01$ compared to the cortex, and $^{\delta}p < 0.01$ compared to the hippocampus of *dl*-MDMA-treated brain regions.

there were no significant gender differences in dopaminergic nerve terminal damage in MDMA-treated mice (Figure 6, lower panel). After 1 week, the density of dopaminergic nerve terminals was reduced by 72% in both male and female +/+ PHS-1-normal mice treated with *d*-MDMA compared to that of the saline-treated controls ($p < 0.001$) (Figure 6, lower panel). In contrast, although *d*-MDMA caused, respectively, 19% and 28% reductions in dopaminergic nerve terminal density in the striatum of −/− female and male PHS-1 knockout mice compared to their genotypically matched saline controls ($p < 0.001$ and $p < 0.001$, respectively), the −/− PHS-1 mice still were substantially protected, exhibiting 2.8-fold (females) and 2.6-fold (males) greater dopaminergic

DOI: 10.1021/cn900022w | ACS Chem. Neurosci. (2010), 1, 366–380

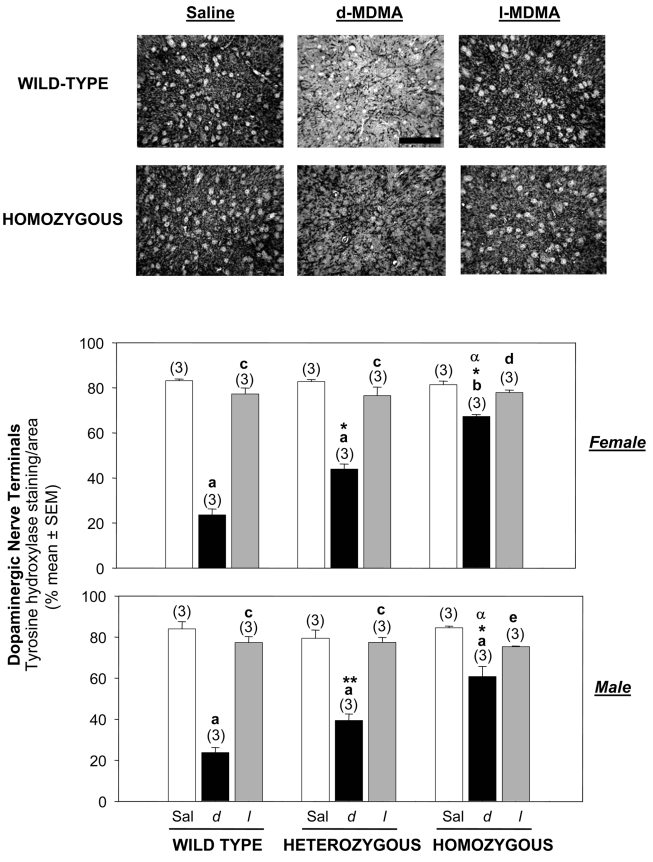

Figure 6. PHS-1 knockout mice are protected against *d*-MDMA-initiated persistent degeneration of dopaminergic nerve terminals in the striatum. Upper panel: *d*- (*d*) or *l*-MDMA (*l*) (10 mg/kg ip) was administered in 4 doses, each given at 2 h intervals. Saline (Sal) vehicle was used as the control. The mice were sacrificed 1 week after the last injection and perfused with 10% formalin. Brain sections were stained for tyrosine hydroxylase indicative of dopaminergic nerve terminals. Immunohistochemical staining is representative of $n = 3$/gender/treatment group; scale bar = 50 μm. Lower panel: quantification of immunohistochemical data reported in the upper panel. The number of animals is given in parentheses. $^{a}p < 0.001$ and $^{b}p < 0.01$ compared to the corresponding saline control for the same PHS-1 genotype; $^{c}p < 0.001$, $^{d}p < 0.05$ and $^{e}p < 0.01$ compared to the corresponding *d*-MDMA-treated PHS-1 genotype; $*p < 0.001$ and $**p < 0.05$ compared to *d*-MDMA-treated wild-type PHS-1-normal mice; $^{\alpha}p < 0.001$ compared to *d*-MDMA-treated heterozygous PHS-1 knockout mice.

density compared to those of the corresponding +/+ PHS-1 mice ($p < 0.001$ and $p < 0.05$, respectively). *d*-MDMA-initiated dopaminergic nerve terminal damage in +/− PHS-1 knockout mice followed a gene dose-dependent pattern similar to that for DNA oxidation, exhibiting an intermediary level of dopaminergic nerve terminal loss compared to the +/+ and −/− mice. In the +/− mice, rostral areas of the striatum were more susceptible to damage compared to caudal areas. Consistent with its inability to enhance DNA oxidation, the *l*-enantiomer of MDMA did not cause damage to the dopaminergic nerve terminal in any PHS-1 genotype.

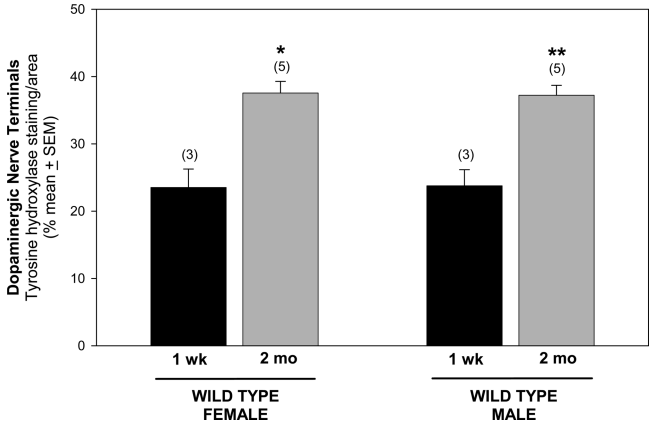

Figure 7. Slight long-term recovery of striatal dopaminergic nerve terminals in wild-type *d*-MDMA-treated PHS-1-normal mice. *d*-MDMA (10 mg/kg ip) was administered in 4 doses, each given at 2 h intervals. The mice were sacrificed 2 months after the last injection and perfused with 10% formalin. Brain sections were stained and quantified for tyrosine hydroxylase (TH), indicative of dopaminergic nerve terminals. The data were plotted as a percentage of TH staining in vehicle-treated wild-type mice (negative control). $*p < 0.04$ and $**p < 0.01$ compared to *d*-MDMA-treated wild-type PHS-1-normal mice sacrificed 1 week after the last injection (10 mg/kg ip). The number of mice is indicated in parentheses.

Assessment of dopaminergic nerve terminals approximately 2 months after *d*-MDMA administration revealed a slight recovery in the range of approximately 37% and 36% in both females and males, respectively, compared to the decrease seen at 1 week (Figure 7). However, the density of dopaminergic nerve terminals observed at 2 months are lower than the density noted in the *d*-MDMA-treated +/− PHS-1 knockout mice 1 week after treatment (Figure 6, lower panel).

MDMA-Initiated Functional Deficits in Motor Coordination Are Abolished in −/− PHS-1 Knockout Mice

The PHS-1 gene dose dependence and stereoselectivity observed for *d*-MDMA-initiated dopaminergic nerve terminal degeneration correlated directly with susceptibility to sustained motor coordination deficits in both females (Figure 8, left) and males (Figure 8, right). Motor deficits were evident within 1 week after the last drug dose and were sustained for at least 4 weeks, in both female and male +/+ PHS-1-normal mice treated with *d*-MDMA compared to their corresponding genotypically matched saline control ($p < 0.001$ and $p < 0.001$, respectively) (Figure 8, upper panel). In contrast, the PHS-1 −/− mice were completely resistant to *d*-MDMA-initiated motor coordination impairment; they were identical to saline controls and substantially different from the gender-matched *d*-MDMA-treated +/+ PHS-1-normal mice (females, $p < 0.001$; males, $p < 0.001$) (Figure 8, top panels).

DOI: 10.1021/cn900022w | ACS Chem. Neurosci. (2010), 1, 366–380

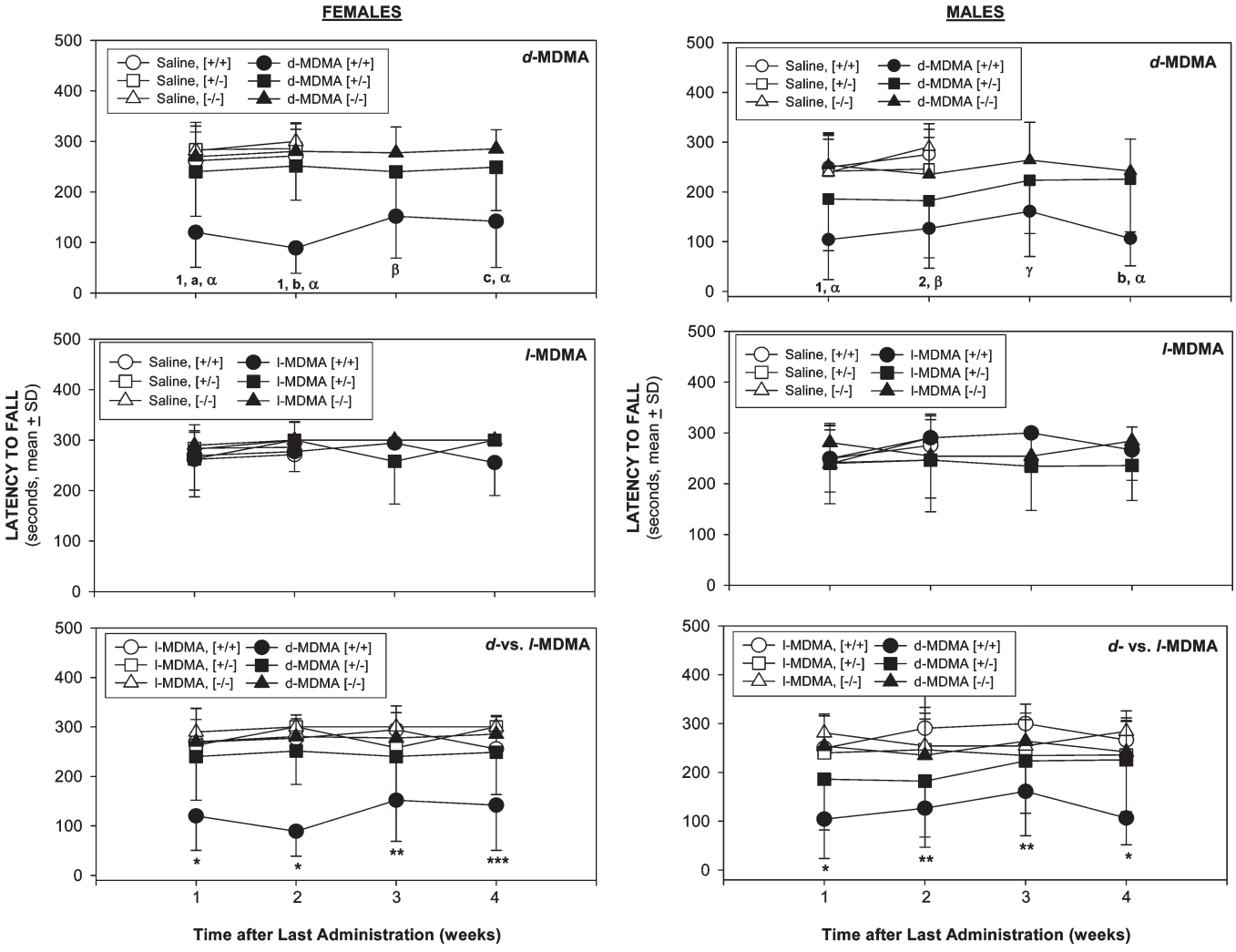

Figure 8. Female and male PHS-1 knockout mice are protected against *d*-MDMA-initiated persistent functional deficits. Motor coordination impairment was assessed by the rotarod test at 25 rpm for mice treated with *d*- or *l*-MDMA or their saline vehicle. The time at which the mice fell from the rod was recorded as the latency. A minimum of 4 mice were used per gender for each group. Left upper panel: *d*-MDMA compared to saline. $^{1}p < 0.001$ compared to its genotypically identical saline control. $^{a}p < 0.003$, $^{b}p < 0.001$, and $^{c}p < 0.04$ compared to *d*-MDMA-treated +/− PHS-1 knockout mice. $^{\alpha}p < 0.001$ and $^{\beta}p < 0.002$ compared to *d*-MDMA-treated −/− PHS-1 knockout mice. Left middle panel: *l*-MDMA compared to saline. No significant differences. Left lower panel: *d*-MDMA compared to its *l*-enantiomer. $*p < 0.001$, $**p < 0.03$, and $***p < 0.02$ compared to *l*-MDMA-treated +/+ PHS-1-normal mice. Right upper panel: *d*-MDMA compared to saline. $^{1}p < 0.001$ and $^{2}p < 0.004$ compared to its genotypically matched saline control. $^{b}p < 0.03$ compared to *d*-MDMA-treated +/− PHS-1 knockout mice. $^{\alpha}p < 0.001$, $^{\beta}p < 0.02$, and $^{\gamma}p < 0.03$ compared to *d*-MDMA-treated −/− PHS-1 knockout mice. Right middle panel: *l*-MDMA compared to saline. No significant differences. Right lower panel: *d*-MDMA compared to its *l*-enantiomer. $*p < 0.001$ and $**p < 0.006$ compared to *l*-MDMA-treated +/+ PHS-1-normal mice.

Although both male and female PHS-1 +/− mice were susceptible to *d*-MDMA-initiated dopaminergic nerve terminal degeneration, these mice were relatively more resistant to the associated functional consequences. Both female and male PHS-1 +/− mice treated with *d*-MDMA consistently exhibited motor coordination performances more deficient than those for the unaffected +/− saline controls or *d*-MDMA-treated −/− PHS-1 knockouts throughout the 4-week period of measurement, although these deficits were not statistically significant. As with dopaminergic nerve terminal damage, *l*-MDMA did not produce motor coordination deficits in any animals tested (Figure 8, middle and bottom panels).

Discussion

Although ROS have been implicated in amphetamine-initiated neurodegeneration, the mechanism is not clear. The hypothesis of amphetamine metabolism via CYP2D6 to redox-cycling quinones, including hepatic formation and transport of a GSH−HHMA conjugate, does not sufficiently explain the neurodegenerative effects of MDMA, nor does the induction of PHS with

DOI: 10.1021/cn900022w | ACS Chem. Neurosci. (2010), 1, 366–380

its associated intrinsic effects. The *in vitro* studies herein using purified PHS and electron paramagnetic resonance spectrometry provide the first direct evidence that PHSs can bioactivate MDMA to a free radical intermediate, as has been shown for other xenobiotics (*31*), including numerous teratogens (*27*) and the neurotoxins MDA and METH (*30*). The further oxidation of 2′-dG to 8-oxo-dG under these *in vitro* conditions shows that MDMA free radicals can initiate the formation of ROS that cause oxidative DNA damage, including 8-oxo-dG formation, consistent with a neurodegenerative potential. The mutagenic role of 8-oxo-dG in cancer is generally appreciated, but this oxidative macromolecular lesion also may affect gene transcription, resulting in neurodegeneration. For example, we recently found that postnatal neurodevelopmental deficits caused by *in utero* exposure to METH are enhanced in knockout mice deficient in oxoguanine glycosylase 1 (OGG1), the major enzyme for repairing 8-oxo-dG (*32*). A similar process may occur in adults exposed to MDMA since METH also is bioactivated by PHSs (*30*). The stereoselective nature of the MDMA-initiated DNA oxidation observed herein is consistent with results from the *in vivo* studies discussed below, as well as with published *in vivo* evidence of stereoselective MDMA, MDA, and METH neurotoxicity residing with the *d*-isomers (*33*). The *in vitro* concentration range for MDMA was chosen for optimal electron paramagnetic resonance (EPR) characterization of PHS-dependent free radical formation, upon the basis of similar studies of teratogens (*29*), and the same concentration was employed for evaluating PHS-dependent DNA oxidation. Complementary studies of the teratogens at lower, clinically relevant concentrations in embryo culture showed similar oxidative DNA damage (*34*), and we have found the same for lower concentrations (100 μM) of MDA and METH in cells stably expressing human PHS-1 (Ramkissoon, A., and Wells, P. G., unpublished work). The *in vivo* studies herein using PHS-1 knockout mice further corroborated the *in vitro* studies, providing direct evidence of a critical role for PHS-1-dependent bioactivation of MDMA in the CNS, including neuroprotection in the −/− PHS-1-deficient mice. Conversely, there was enhanced DNA oxidation in +/+ PHS-1-normal mice, but among different brain regions, the level of PHS-1 protein expression correlated positively with the severity of MDMA-enhanced DNA oxidation in each region. This oxidative DNA damage in several relevant brain regions correlated directly with long-lasting neurodegenerative cellular changes and functional motor coordination deficits, both of which were reduced in +/− PHS-1 knockout mice and abolished in −/− mice. Furthermore, DNA oxidation and persistent nerve terminal degeneration and functional deficits were restricted to the *d*-enantiomer of MDMA, consistent with the *in vitro* results. Stereoselective affinity of brain dopamine (DA) transporters for the *d*-enantiomer of MDMA (*35*, *36*) may also contribute to the stereoselectivity of neurotoxicity. However, as shown herein, MDMA is directly bioactivated by PHS to a potentially neurotoxic free radical intermediate, and its neurotoxicity is not necessarily dependent upon transporter-dependent uptake or DA release. The *in vitro* demonstration of PHS-1-dependence and stereoselectivity in the formation of an MDMA free radical and subsequent DNA oxidation, together with the *in vivo* stereoselective nature of oxidative DNA damage and PHS-1 gene dose-dependence, provides the first direct evidence for PHS-catalyzed bioactivation of MDMA to a free radical intermediate that initiates DNA oxidation and subsequent functional deficits.

Remarkably, regional differences in DNA oxidation were observed at higher levels in selective brain regions associated with motor function, specifically the striatum and substantia nigra. The correlation of increasing PHS-1 levels with an increasing severity of oxidative DNA damage among different brain regions is consistent with results from other studies using the structurally related drugs MDA and METH (*30*). A similar process may occur with endogenous DNA damage since among different brain regions, there was a high correlation between the amount of endogenous DNA oxidation and the amount of enhanced damage that occurred with MDMA exposure. Part of the endogenous oxidative DNA damage may be due to PHS-catalyzed bioactivation of endogenous brain substrates since *in vitro* studies in our laboratory have found that several neurotransmitters as well as their precursors and metabolites produce PHS-dependent DNA oxidation (*37*), which may play a role in neurodegeneration associated with aging. This hypothesis is consistent with the observed positive correlation between constitutive PHS-1 protein levels and endogenous DNA oxidation in both +/+ and +/− mice. These correlations suggest that the balance between PHS-catalyzed bioactivation and protective antioxidative and/or DNA repair pathways may be an important determinant of target tissues and risk for neurodegeneration.

The stereoselective potency of the *d*-enantiomers of MDMA in enhancing DNA oxidation observed in our *in vitro* and *in vivo* studies reflects other stereoselective outcomes seen *in vitro* and *in vivo* in rats and humans (*33*, *38*). While the *d*-enantiomer has been shown to be more potent than the *l*-enantiomer with respect to receptor-mediated pharmacological effects, it was not known whether there was stereoselectivity in the PHS-1-catalyzed bioactivation and neurodegenerative effects of MDMA. We show herein that PHS-1 indeed does exhibit stereoselectivity for MDMA bioactivation. Accordingly, arachidonate-dependent, PHS-catalyzed

DOI: 10.1021/cn900022w | *ACS Chem. Neurosci.* (2010), *1*, 366–380

bioactivation of MDMA provides a new mechanism for this stereoselectivity unrelated to P450-catalyzed metabolism, differential dopaminergic receptor binding, or reuptake affinity. The stereoselective enhancement in ROS-mediated DNA oxidation by *d*-MDMA compared to its *l*-isomer may be due in part to its increased affinity for PHS-1, as has been observed with cytochrome P450 (*15*). Most importantly, the *in vitro* stereoselective potency of *d*-MDMA over *l*-MDMA was also observed *in vivo* with respect to MDMA-initiated DNA oxidation, dopaminergic nerve terminal degeneration and functional deficits in +/+ PHS-1-normal mice, all of which were abolished in PHS-1 −/− knockout mice. The persistence of nerve terminal degeneration and functional deficits for at least 4 weeks after treatment with *d*-MDMA but not its *l*-isomer provides the most definitive evidence to date for a stereoselective determinant in the irreversible neurodegenerative effects of MDMA.

The biochemical pathway summarized in Supporting Information, Figure S4 could account for ROS generation characteristic of MDMA neurotoxicity, as has been previously postulated for several teratogens (*29*). During this process, hydroperoxides of MDMA can generate ROS which, in the absence of adequate cytoprotection, can oxidize cellular macromolecules, leading to neuronal injury.

In biological responses to external stimuli, PHS-1 knockout mice show gene dosage effects, with heterozygous knockouts being intermediate between null and wild-type mice (*39*). Our studies herein parallel this PHS-1 gene dosage effect for MDMA-initiated DNA oxidation, nerve terminal degeneration, and motor coordination deficits, with PHS-1 +/− mice being partially protected at least from neuronal degeneration compared to +/+ PHS-1-normal mice, but not fully protected compared to homozygous null mice. Although the heterozygotes were not also significantly protected from MDMA-initiated motor coordination deficits based upon statistical analysis, the observed biological pattern wherein both males and females consistently exhibited lower function than +/+ PHS-1-normal mice for all time points suggests that the heterozygous genotype likely confers intermediate protection for this parameter as well.

The PHS-1 −/− mice treated with *d*-MDMA were substantially but not fully protected against dopaminergic nerve terminal degeneration. Although PHS-1 −/− mice do not compensate by up-regulating PHS-2 protein expression or vice versa (*40*−*42*), it is possible that constitutive PHS-2 contributed to the residual *d*-MDMA bioactivation and nerve terminal degeneration observed in the PHS-1 −/− knockouts. This would be consistent with the apparent contribution of constitutive PHS-2 to endogenous oxidative DNA damage, which for any given brain region was similar in untreated +/+, +/−, and −/− mice. If so, then regional expression of both PHS-1 and PHS-2 and modulation of particularly the latter isozyme by environmental factors, may play variable roles in the mechanism of MDMA nerve terminal degeneration. Following initial MDMA treatment, DNA oxidation appears to be due primarily to PHS-1-catalyzed bioactivation, particularly in brain regions where PHS-2 is nonconstitutive. After repetitive MDMA administration, PHS-2 may be induced in selective brain regions, which in those tissues could contribute to MDMA bioactivation and nerve terminal degeneration. For example, the structurally related amphetamine, METH, can induce striatal PHS-2 protein expression within 72 h (*43*). PHS induction also is commonly associated with various diseases, including cancer, Alzheimer's disease, and other neurodegenerative diseases (*44*, *45*), which in induced cells could enhance the bioactivation of endogenous substrates or xenobiotics such as MDMA to toxic free radical intermediates. Although homozygous PHS-1 knockout mice were not completely protected against *d*-MDMA-initiated neuronal degeneration at the ultrastructural level, their functional motor coordination was not measurably affected. This perhaps is not surprising since *d*-MDMA-treated homozygous *null* mice only had a 19 to 28% reduction of striatal dopaminergic neuronal density. In humans, the clinical manifestations of motor impairment symptoms associated with Parkinson's disease occur only after the nigro-striatal dopaminergic neuronal population has been depleted by 80% (*46*). Even the heterozygous PHS-1 knockout mice, in which *d*-MDMA caused a 47 to 53% dopaminergic neuronal depletion, did not exhibit significant motor coordination deficits, although a consistent trend was observed.

Since there is no evidence of any functional recovery at 1 month, it appears that even up to a 37% recovery of dopaminergic nerve terminals (seen at 2 months) in *d*-MDMA-treated +/+ PHS-1-normal mice, assuming they are biochemically functional, is not adequate to restore normal motor coordination. Alternatively, upon the basis of studies of MDA and METH that showed motor coordination deficits extending at least 6 months after treatment (*30*), these partially recovered nerve terminals and/or their associated neurons may not be biochemically normal. It also is possible that additional, more persistent molecular lesions may contribute to the observed motor coordination deficits.

Gender differences are evident in several neurodegenerative diseases. Alzheimer's disease is more prevalent in women than in men (*47*), while Parkinson's disease is more prevalent in men (*48*). We found no gender differences in DNA oxidation, dopamine nerve terminal damage, or motor deficits with any MDMA stereoisomer or PHS-1 genotype tested, although there

DOI: 10.1021/cn900022w | *ACS Chem. Neurosci.* (2010), *1*, 366–380

are numerous contradictory gender studies of amphetamine effects (*49*−*51*). Our study indicates that gender specificity is not apparent in any of the steps in the process of MDMA neurodegeneration in mice, including PHS-catalyzed bioactivation, ROS-mediated oxidative DNA damage, nerve terminal degeneration, and motor coordination deficits. Gender differences reported in other amphetamine studies may be due in part to outcomes modulated by differences in estrogen levels between females and males (*52*) that may be age-, species-, or strain-dependent and more particularly, due to the measurement of outcomes that do not reflect molecular and functional changes involved in long-lasting nerve terminal degeneration confirmed weeks to months after the last drug treatment.

Higher doses of MDMA cause hyperthermia, which has been implicated in the mechanism of its neurotoxicity. However, in this study of long-term neurodegenerative effects following acute exposure to MDMA, it is unlikely that hyperthermia played a substantial modulatory role. Most directly, acute hyperthermia is unlikely to vary among PHS genotypes, and PHS-dependent bioactivation and DNA oxidation also occurred *in vitro*, where the temperature was constant. Also, lower doses of MDMA that do not cause hyperthermia are still neurotoxic. Perhaps more relevant to the current study, inhibition of hyperthermia does not consistently block the neurotoxic effects of MDMA, and conversely, the neurotoxicity of MDMA can be inhibited without modifying its hyperthermic effect (*2*, *53*−*56*).

PHS-1 and PHS-2 have been localized to the lumenal surfaces of the endoplasmic reticulum and the inner and outer membranes of the nuclear envelope (*57*), of which the latter would be particularly conducive for catalyzing the bioactivation of MDMA and related amphetamines, as well as endogenous substrates, to free radical intermediates that enhance DNA oxidation. The resistance of PHS-1 *null* mice to the neurodegenerative effects of MDMA herein is consistent with complementary studies of the MDMA metabolite MDA showing protection against both nerve terminal degeneration and functional deficits by pretreatment with a single dose of the PHS inhibitor acetylsalicylic acid (*30*). Furthermore, we confirm that oxidative damage to DNA may be an early macromolecular lesion involved in the initiation of amphetamine-induced neurotoxicity. These results, together with the observed stereoselectivity of MDMA bioactivation, suggest that the free radical intermediates characterized for the amphetamines are relevant to their molecular mechanism of neuronal damage, which may involve oxidative damage to nuclear and/or mitochondrial DNA. Although this study focused upon the neurodegenerative role of oxidative DNA damage, the results do not preclude the possibility of complementary or concomitant pathological roles for oxidative damage to other cellular macromolecules (RNA, protein, and lipids) or for enhanced ROS-mediated signal transduction. Oxidative DNA damage and the resultant gene modifications, which can disrupt transcription, translation, and DNA replication, are associated with increased age (*58*), neurodegenerative diseases (*59*), and ROS-initiating xenobiotics and can ultimately result in mutations, altered cellular function, and/or cell death. This was evident herein with the protection against MDMA-initiated ROS-mediated DNA oxidation in the brains of PHS-1 −/− mice, which prevented the degeneration of dopaminergic neurons and associated functional motor deficits. The evidence herein for damage to monoaminergic neurons, which alters normal motor and possibly cognitive function (*60*−*62*), is consistent with the speculation that amphetamines may contribute to a variety of neurodegenerative diseases and conditions such as Parkinson's disease and depression.

In summary, our *in vitro* studies provide the first direct evidence that MDMA is bioactivated by PHS-1 to free radical intermediates that initiate ROS-mediated DNA oxidation. The stereoselective nature of PHS-dependent oxidative DNA damage was similar to that observed in our *in vivo* studies of amphetamine-initiated macromolecular damage and nerve terminal degeneration in PHS-1 wild-type mice, which are abolished in PHS-1 *null* mice, confirming the potential relevance of this novel mechanism. PHS-dependent bioactivation of substrates within the brain, as implicated herein with MDMA, may constitute a common molecular mechanism for neurodegeneration caused by ROS-initiating xenobiotics and possibly endogenous substrates.

Methods

Chemicals

Purified PHS-1 and 8-hydroxy-2′-deoxyguanosine were obtained from Cayman Chemical Co. (Ann Arbor, MI). Arachidonic acid, hematin, α-phenyl-*N*-*t*-butylnitrone (PBN), 2′-deoxyguanosine, nuclease P1, and *Escherichia coli* alkaline phosphatase were obtained from Sigma-Aldrich (Oakville, Canada). Redistilled phenol was from Aldrich Chemical Co. (Oakville, ON, Canada), chloroform/isoamyl alcohol/phenol (CIP, 24:1:25) from Life Technologies, Inc. (Burlington, ON, Canada), and proteinase K and complete, Mini, EDTA-free protease inhibitor cocktail tablets from Roche Diagnostics (Laval, QC, Canada). 5,8,11,14-Eicosatetraynoic acid (ETYA) was a gift from Hoffmann-La Roche Ltd. (Etobicoke, ON, Canada). PCR primers were purchased from ACGT Corporation (Toronto, ON, Canada). Taq polymerase and dNTPs were purchased from Perkin-Elmer (Mississauga, ON, Canada). All other reagents used were of analytical or HPLC grade.

Drugs

Pure racemic (*dl*-), *d*-, and *l*-isomers of MDMA were provided by the Research Technology Branch of the National Institute on Drug Abuse (Rockville, MD).

DOI: 10.1021/cn900022w | *ACS Chem. Neurosci.* (2010), *1*, 366–380

PHS-1 Knockout Mouse Colony and Genotyping

Heterozygous (+/−)-PHS-1 knockout male mice of the 129/B6 strain were provided by Dr. Robert Langenbach (NIEHS, Research Triangle Park, North Carolina) (*40*). These males outbred to CD-1 female mice (Charles River Canada, St. Constant, QC, Canada) to generate F1 129/B6/CD-1 offspring. The colony obtained was further inbred by mating littermates for 7 subsequent generations. F8 litters of female and male PHS-1 mice were tested for susceptibility to MDMA-initiated neurodegeneration at 3−4 months of age. The male to female ratio was 50:50, and the PHS-1 genotypes followed a Mendelian ratio. Mice were housed in plastic cages with ground corn-cob bedding (Beta Chip; Northeastern Products, Warrensburg, New York) and maintained in temperature-controlled rooms with a 12-h light−dark cycle. Food (Laboratory Rodent Chow 5001; Ralston Purina, Strathroy, ON, Canada) and tap water were provided *ad libitum*. All PHS-1 genotypes were confirmed as previously described (*63*). The animal studies were approved by the University of Toronto Animal Care Committee in accordance with the Guidelines of the Canadian Council on Animal Care.

In Vitro Bioactivation of MDMA to Free Radical Reactive Intermediates by PHS-1

PHS-1 (1000 units/mL) was incubated with hematin (1.0 μM) and phenol (0.5 mM) for 1 min at 37 °C in 80 mM potassium phosphate buffer at pH 7.9. After the addition of *dl*-MDMA (500 μM or 1 mM) or phenytoin (PHT, 0.25 mM and 0.5 mM), or their vehicle and the free radical spin trap PBN (1 mM), arachidonic acid (67 μM) was subsequently added to initiate the reaction. After incubation for 1−10 min at 37 °C, reactions were terminated and extracted with 2 mL of ethyl acetate. The ethyl acetate layer was then completely reduced under nitrogen, reconstituted with 300 μL of ethyl acetate, and analyzed by EPR spectrometry for free radical adducts as previously described (*29*). To block PHS-1-mediated bioactivation of *dl*-MDMA, the PHS inhibitor ETYA (40 μM) was incubated with the PHS-1 enzyme at 37 °C for 1 min prior to the addition of MDMA and arachidonic acid.

Oxidation of 2′-Deoxyguanosine (2-′dG)

2′-Deoxyguanosine (2′-dG) (1 mg) was incubated with or without MDMA in the presence of PHS-1 using the conditions mentioned above with the following alterations: PBN was replaced with 2′-dG, and a higher concentration of arachidonic acid (140 μM) was used to start the reaction. The resulting mixture was filtered (0.22 μm), and the filtrate was analyzed for 8-oxo-2′deoxyguanosince (8-oxo-dG) by high-performance liquid chromatography coupled with electrochemical detection (HPLC-EC) (*64*). Samples were injected in duplicate.

Animal Treatment and Analysis for DNA Oxidation

Drugs were dissolved with sterilized 0.9% saline, and the drug or its saline vehicle was injected intraperitoneally (ip) in a fixed volume of 0.1 mL/10 g body weight. Female and male PHS-1 wild-type (+/+), heterozygous (+/−), or homozygous (−/−) mice were administered 4 doses of *dl*-, *d*-, or *l*-MDMA (10 mg/kg) or 0.9% saline (vehicle), with each dose given at 2 h intervals. The mice were anesthetized by isofluorane and sacrificed at various time points. For DNA oxidation, the brains were isolated, rinsed in ice cold 1.15% KCl solution, and subsequently microdissected on ice to obtain the cortex, hippocampus, striatum, substantia nigra, brainstem, and cerebellum. Dissected brain regions were snap-frozen in liquid nitrogen and stored at −80 °C until analyzed as described elsewhere (*64*). For immunohistochemistry, mice were perfused with PBS, followed by 10% formalin. Brains were subsequently fixed in 10% formalin. DNA oxidation was quantified by HPLC-EC as previously described (*64*, *65*).

Immunoblotting

A 10−30% homogenate was prepared with microdissected brain tissue in RIPA buffer (1% NP-40, 0.5% Na^+ deoxycholate, and 0.1% SDS in PBS) supplemented with Complete, Mini, EDTA-free protease inhibitor cocktail tablets (Roche Diagnostics). The homogenate was allowed to lyse for 3 h at 4 °C and subsequently centrifuged for 10 min at 16,000*g*. The supernatant was quantified for total cellular protein using the modified Lowry Assay (*66*). An 80 μg sample of cellular protein was separated using a 12% SDS−PAGE gel under reducing and denaturing conditions and transferred onto a nitrocellulose membrane (Bio-Rad Laboratories, Hercules, CA). Equal protein loading was confirmed by Ponceau S staining. PHS-1 was detected with rabbit polyclonal antiserum against PHS-1 (diluted 1:500, Caymen Chemicals, Ann Arbor, MI) and goat antirabbit IgG-horseradish peroxidase (diluted 1:5000, Santa Cruz Biotechnologies Inc., Santa Cruz, CA). Peroxidase activity was visualized by an enhanced chemiluminescence (ECL) detection system (Amersham Biosciences, Piscataway, NJ).

Immunohistochemistry

Brain sections (5 μm) were deparaffinized in xylene and ethanol, followed by a high temperature unmasking in 0.01 M sodium citrate buffer (pH 6.0) for 5 min. Tissue sections were blocked for at least 2 h with 3% BSA, 20 mM $MgCl_2$, 0.3% Tween 20, and 5% goat serum in PBS followed by an overnight incubation with the goat antirabbit tyrosine hydroxylase primary antibody (1:600, Chemicon International Inc., Temecula, CA). Sections were incubated with biotinylated goat antirabbit IgG reagent (1:200, Vector Laboratories, Burlington, ON, Canada) and detection was performed using the Vectastain Elite ABC Reagent kit and DAB kit (Vector Laboratories) according to the manufacturer's specifications.

Quantitation of Immunoblot and Immunohistochemical Data

Determination of protein level and immunohistochemical staining was performed using the NIH Imaging freeware (Scion v4.02). A representative value was taken from the means of the integrated density acquired from three independently obtained measurements from each sample, with a minimum of $n = 3$/gender/treatment group.

For Western blots, a representative value was taken from the means of the integrated density acquired from three independently obtained measurements from each sample; with a minimum of $n = 6$/treatment group. For immunohistochemistry, the density of surviving dopamine axon terminals per square millimeter of tissue area in tyrosine hydroxylase immunoreactive-stained (TH-IR) sections was used as an index of striatal density of TH innervation and was measured in coronal sections in the caudate putamen of

DOI: 10.1021/cn900022w | *ACS Chem. Neurosci.* (2010), *1*, 366–380

the striatum. Quantification of TH-IR neurons within a unit area of tissue was conducted using a Leitz DMIL inverted microscope (Leica Microsystems Inc., Richmond Hill, ON, Canada) equipped with a Nikon COOLPIX 995 (Nikon Corporation, Mississauga, ON, Canada). Digital images were made in a standard frame sample area taken at 400× magnification. TH-IR was assessed using counts of TH-stained neuropil labeled above the threshold. The threshold was set at the same level for each section sampled. To minimize variations attributed to morphometric analysis associated with immunohistochemical staining and in the quantification technique, three different coronal sections were employed for measurements in each PHS-1-normal, heterozygous, or homozygous PHS-1 knockout mouse treated with (a) saline; (b) *d*-MDMA; or (c) *l*-MDMA. For each section, 9 fields within the caudate putamen were analyzed bilaterally. Thus, for one mouse, the analysis of 3 separate coronal sections gave rise to a representative value taken from the means of the integrated density acquired from 54 ($3 \times 9 \times 2$) independently obtained measurements. This value was then divided by the unit area of tissue and the result expressed as a percentage. Quantification of tissue staining was performed in a blinded fashion using experimental codes such that animal treatments were not known during measuring.

Behavioral Studies

Female and male PHS-1-normal, heterozygous, or homozygous PHS-1 knockout mice were treated with *d*- or *l*-MDMA or saline one week before the assessment of behavioral motor coordination using the rotarod test. Male and female mice were given 60 min to adjust to their new surroundings followed by trial conditioning and training on a constant speed rotarod (rod diameter = 3.6 cm). Briefly, mice were required to perch on the stationary rod for 30 s to accustom themselves before being allowed to run with a constant speed of 5 rpm for 90 s. Mice that succeeded 3 trials (2 h intervals) without falling were tested. Mice were tested for motor coordination at a constant speed of 5 rpm for 90 s, then gradually increasing to a constant speed of 20−30 rpm for a maximum of 5 min. The performance time and speed at which the mice fell from the rod were recorded.

Statistical Analysis

Statistical significance of differences between paired data was determined by the two-tailed Student's *t* test, while multiple comparisons among groups were analyzed by the one-way analysis of variance (ANOVA) with a subsequent Tukey's test (GraphPad InStat 3.05, GraphPad Software, Inc., San Rafael, CA). For data with two independent variables, two-way ANOVA was performed followed by a Bonferroni post-test when F ratios were significant. The level of significance was determined to be at $p < 0.05$.

Supporting Information Available

Postulated bioactivation of xenobiotics to a neurodegenerative free radical intermediate by prostaglandin H synthase and/or other peroxidases; differences in constitutive PHS-1 protein expression in different brain regions; relationship of PHS-1 protein expression and constitutive DNA oxidation in different brain regions of PHS-1 wild-type and heterozygous mice; and postulated mechanism for prostaglandin H synthase-catalyzed bioactivation of amphetamines. This material is available free of charge via the Internet at http://pubs.acs.org.

Author Information

Corresponding Author

* Corresponding author. Faculty of Pharmacy, University of Toronto, 144 College St., Toronto, Ontario, Canada M5S 3M2. Tel: 416-978-3221. Fax: 416-267-7797. E-mail: pg.wells@utoronto.ca.

Present Addresses

§ Current address: Drug Safety Evaluation Projects, Sanofi-Aventis US Inc., Bridgewater, NJ 08807.

Funding Sources

These studies were supported by a grant from the Canadian Institutes of Health Research (CIHR). W.J. was supported by a doctoral award from the CIHR/Rx&D Health Research Foundation and the Covance doctoral fellowship from the Society of Toxicology.

Notes

Preliminary reports of this research were presented at the 2001 and 2003 annual meetings of the Society of Toxicology (U.S.A.) [*Toxicol. Sci.* (Supplement: The Toxicologist) 60(S-1): 368 (No. 1752), 2001; and 72(S-1): 72 (No. 350), 2003].

Acknowledgment

We thank Drs. Toufan Parman, Frank Di Cosmo, and Guoman Chen for their consultations in the EPR studies and Wanda Newerly and Dr. John Roder for their consultations in the behavioural studies.

Abbreviations

CYP, cytochromes P450; ETYA, eicosatetraynoic acid; HFSC, hyperfine splitting constant; HPLC-EC, high-performance liquid chromatography-electrochemical detection; METH, methamphetamine; MDA, 3,4-methylenedioxyamphetamine; MDMA, 3,4-methylenedioxymethamphetamine; 8-oxo-dG, 8-oxo-2′-deoxyguanosine; PBN, α-phenyl-*N*-*t*-butylnitrone; PHS, prostaglandin H synthase; ROS, reactive oxygen species; TH, tyrosine hydroxylase.

References

1. Nichols, D. E. (1986) Differences between the mechanism of action of MDMA, MBDB, and the classic hallucinogens. Identification of a new therapeutic class: entactogens. *J. Psychoactive Drugs 18*, 305–313.

2. Broening, H. W., Bowyer, J. F., and Slikker, W. (1995) Age-dependent sensitivity of rats to the long-term effects of

DOI: 10.1021/cn900022w | *ACS Chem. Neurosci.* (2010), *1*, 366–380

the serotonergic neurotoxicant (±)-3,4-methylenedioxymethamphetamine (MDMA) correlates with the magnitude of the MDMA-induced thermal response. *J. Pharmacol. Exp. Ther. 275*, 325–333.

3. Kalant, H. (2001) The pharmacology and toxicology of "ecstasy" (MDMA) and related drugs. *CMAJ 165*, 917–928.

4. Bolla, K. I., McCann, U. D., and Ricaurte, G. A. (1998) Memory impairment in abstinent MDMA ("Ecstasy") users. *Neurology 51*, 1532–1537.

5. McGuire, P. (2000) Long term psychiatric and cognitive effects of MDMA use. *Toxicol. Lett. 112−113*, 153–156.

6. Zakzanis, K. K., and Young, D. A. (2001) Memory impairment in abstinent MDMA ("Ecstasy") users: a longitudinal investigation. *Neurology 56*, 966–969.

7. Cadet, J. L., and Brannock, C. (1998) Free radicals and the pathobiology of brain dopamine systems. *Neurochem. Int. 32*, 117–131.

8. McCann, U. D., Szabo, Z., Scheffel, U., Dannals, R. F., and Ricaurte, G. A. (1998) Positron emission tomographic evidence of toxic effect of MDMA ("Ecstasy") on brain serotonin neurons in human beings. *Lancet 352*, 1433–1437.

9. Obrocki, J., Buchert, R., Vaterlein, O., Thomasius, R., Beyer, W., and Schiemann, T. (1999) Ecstasy--long-term effects on the human central nervous system revealed by positron emission tomography. *Br. J. Psychiatry 175*, 186–188.

10. Hatzidimitriou, G., McCann, U. D., and Ricaurte, G. A. (1999) Altered serotonin innervation patterns in the forebrain of monkeys treated with (±)3,4-methylenedioxymethamphetamine seven years previously: factors influencing abnormal recovery. *J. Neurosci. 19*, 5096–5107.

11. Ali, S. F., Newport, G. D., Scallet, A. C. Z. B., Ferguson, S. A., Bailey, J. R., Paule, M. G., and Slikker, W. (1993) Oral administration of 3,4-methylenedioxymethamphetamine (MDMA) produces selective serotonergic depletion in the nonhuman primate. *Neurotoxicol. Teratol. 15*, 91–96.

12. Slikker, W., Ali, S. F., Scallet, A. C., Frith, C. H., Newport, G. D., and Bailey, J. R. (1988) Neurochemical and neurohistological alterations in the rat and monkey produced by orally administered methylenedioxymethamphetamine (MDMA). *Toxicol. Appl. Pharmacol. 94*, 448–457.

13. Green, A. R., Mechan, A. O., Elliott, J. M., O'Shea, E., and Colado, M. I. (2003) The pharmacology and clinical pharmacology of 3,4-methylenedioxymethamphetamine (MDMA, "ecstasy"). *Pharmacol. Rev. 55*, 463–508.

14. Colado, M. I., O'Shea, E., Esteban, B., Granados, R., and Green, A. R. (1999) In vivo evidence against clomethiazole being neuroprotective against MDMA ('ecstasy')-induced degeneration of rat brain 5-HT nerve terminals by a free radical scavenging mechanism. *Neuropharmacology 38*, 307–314.

15. Tucker, G. T., Lennard, M. S., Ellis, S. W., Woods, H. F., Cho, A. K., Lin, L. Y., Hiratsuka, A., Schmitz, D. A., and Chu, T. Y. (1994) The demethylenation of methylenedioxymethamphetamine ("ecstasy") by debrisoquine hydroxylase (CYP2D6). *Biochem. Pharmacol. 47*, 1151–1156.

16. Monks, T. J., Jones, D. C., Bai, F., and Lau, S. S. (2004) The role of metabolism in 3,4-(±)-Methylenedioxyamphetamine and 3,4-(±)-methylenedioxymethamphetamine (Ecstasy) toxicity. *Ther. Drug Monit. 26*, 132–136.

17. de la Torre, R., Farre, M., Roset, P. N., Pizarro, N., Abanades, S., Segura, M., Segura, J., and Cami, J. (2004) Human pharmacology of MDMA: pharmacokinetics, metabolism and disposition. *Ther. Drug Monit. 26*, 137–144.

18. Warner, M., Hellmold, H., Yoshida, S., Liao, D., Hedlund, E., and Gustafsson, J. A. (1997) Cytochrome P450 in the breast and brain: role in tissue-specific activation of xenobiotics. *Mutat. Res. 376*, 79–85.

19. Sasame, H. A., Ames, M. M., and Nelson, S. D. (1977) Cytochrome P-450 and NADPH cytochrome c reductase in rat brain: formation of catechols and reactive catechol metabolites. *Biochem. Biophys. Res. Commun. 78*, 919–926.

20. Brady, J. F., Di Stefano, E. W., and Cho, A. K. (1986) Spectral and inhibitory interactions of (±)-3,4-methylenedioxyamphetamine (MDA) and (±)-3,4-methylenedioxymethamphetamine (MDMA) with rat hepatic microsomes. *Life Sci. 39*, 1457–1464.

21. Pelkonen, O., Maenpaa, J., Taavitsainen, P., Rautio, A., and Raunio, H. (1998) Inhibition and induction of human cytochrome P450 (CYP) enzymes. *Xenobiotica 28*, 1203–1253.

22. Warner, M., and Gustafsson, J. A. (1994) Effect of ethanol on cytochrome P450 in the rat brain. *Proc. Natl. Acad. Sci. U.S.A. 91*, 1019–1023.

23. Colado, M. I., Williams, J. L., and Green, A. R. (1995) The hyperthermic and neurotoxic effects of 'Ecstasy' (MDMA) and 3,4 methylenedioxyamphetamine (MDA) in the dark Agouti (DA) rat, a model of the CYP2D6 poor metabolizer phenotype. *Br. J. Pharmacol. 115*, 1281–1289.

24. Parman, T., and Wells, P. G. (2002) Embryonic prostaglandin H synthase-2 (PHS-2) expression and benzo[a]pyrene teratogenicity in PHS-2 knockout mice. *FASEB J. 16*, 1001–1009.

25. Parman, T., Wiley, M. J., and Wells, P. G. (1999) Free radical-mediated oxidative DNA damage in the mechanism of thalidomide teratogenicity. *Nat. Med. 5*, 582–585.

26. Wells, P. G., Kim, P. M., Laposa, R. R., Nicol, C. J., Parman, T., and Winn, L. M. (1997) Oxidative damage in chemical teratogenesis. *Mutat. Res. 396*, 65–78.

27. Wells, P. G., McCallum, G. P., Chen, C. S., Henderson, J. T., Lee, C. J. J., Perstin, J., Preston, T. J., Wiley, M. J., and Wong, A. W. (2009) Oxidative stress in developmental origins of disease: teratogenesis, neurodevelopmental deficits and cancer. *Toxicol. Sci. 108*, 4–18.

28. Wells, P., Kim, P., Nicol, C., Parman, T., and Winn, L. (1997) Reactive Intermediates, in *Drug Toxicity in Embryonic Development* (Kavlock, R., and Daston, D., Eds.) pp 453−518, Springer-Verlag, Heidelberg, Germany.

29. Parman, T., Chen, G., and Wells, P. G. (1998) Free radical intermediates of phenytoin and related teratogens. Prostaglandin H synthase-catalyzed bioactivation, electron paramagnetic resonance spectrometry, and photochemical product analysis. *J. Biol. Chem. 273*, 25079–25088.

DOI: 10.1021/cn900022w | *ACS Chem. Neurosci.* (2010), *1*, 366–380

30. Jeng, W., Ramkissoon, A., Parman, T., and Wells, P. G. (2006) Prostaglandin H synthase-catalyzed bioactivation of amphetamines to free radical intermediates that cause CNS regional DNA oxidation and nerve terminal neurodegeneration. *FASEB J. 20*, 638–650.

31. Eling, T. E., Thompson, D. C., Foureman, G. L., Curtis, J. F., and Hughes, M. F. (1990) Prostaglandin H synthase and xenobiotic oxidation. *Annu. Rev. Pharmacol. Toxicol. 30*, 1–45.

32. Wong, A. W., McCallum, G. P., Jeng, W., and Wells, P. G. (2008) Oxoguanine glycosylase 1 (OGG1) protects against methamphetamine-enhanced fetal brain oxidative DNA damage and neurodevelopmental deficits. *J. Neurosci. 28*, 9047–9054.

33. O'Callaghan, J. P., and Miller, D. B. (1994) Neurotoxicity profiles of substituted amphetamines in the C57BL/6J mouse. *J. Pharmacol. Exp. Ther. 270*, 741–751.

34. Winn, L. M., and Wells, P. G. (1995) Phenytoin-initiated DNA oxidation in murine embryo culture, and embryo protection by the antioxidative enzymes superoxide dismutase and catalase: evidence for reactive oxygen species-mediated DNA oxidation in the molecular mechanism of phenytoin teratogenicity. *Mol. Pharmacol. 48*, 112–120.

35. Baumann, M. H., Wang, X., and Rothman, R. B. (2007) 3,4-Methylenedioxymethamphetamine (MDMA) neurotoxicity in rats: a reappraisal of past and present findings. *Psychopharmacology 189*, 407–424.

36. Johnson, M. P., Hoffman, A. J., and Nichols, D. E. (1986) Effects of the enantiomers of MDA, MDMA and related analogues on [3H]serotonin and [3H]dopamine release from supeffused rat brain slices. *Eur. J. Pharmacol. 132*, 269–276.

37. Goncalves, L. L., Ramkissoon, A., and Wells, P. G. (2009) Prostaglandin H synthase-1-catalyzed bioactivation of neurotransmitters, their precursors and metabolites: oxidative DNA damage and electron spin resonance spectroscopy studies. *Chem. Res. Toxicol. 22*, 842–852.

38. Schmidt, C. J., Levin, J. A., and Lovenberg, W. (1987) In vitro and in vivo neurochemical effects of methylenedioxymethamphetamine on striatal monoaminergic systems in the rat brain. *Biochem. Pharmacol. 36*, 747–755.

39. Langenbach, R., Loftin, C., Lee, C., and Tiano, H. (1999) Cyclooxygenase knockout mice: models for elucidating isoform-specific functions. *Biochem. Pharmacol. 58*, 1237–1246.

40. Langenbach, R., Morham, S. G., Tiano, H. F., Loftin, C. D., Ghanayem, B. I., Chulada, P. C., Mahler, J. F., Lee, C. A., Goulding, E. H., and Kluckman, K. D.; et al. (1995) Prostaglandin synthase 1 gene disruption in mice reduces arachidonic acid-induced inflammation and indomethacin-induced gastric ulceration. *Cell 83*, 483–492.

41. Dinchuk, J. E., Car, B. D., Focht, R. J., Johnston, J. J., Jaffee, B. D., Covington, M. B., Contel, N. R., Eng, V. M., Collins, R. J., and Czerniak, P. M.; et al. (1995) Renal abnormalities and an altered inflammatory response in mice lacking cyclooxygenase II. *Nature 378*, 406–409.

42. Morham, S. G., Langenbach, R., Loftin, C. D., Tiano, H. F., Vouloumanos, N., Jennette, J. C., Mahler, J. F., Kluckman, K. D., Ledford, A., and Lee, C. A.; et al. (1995) Prostaglandin synthase 2 gene disruption causes severe renal pathology in the mouse. *Cell 83*, 473–482.

43. Kita, T., Shimada, K., Mastunari, Y., Wagner, G. C., Kubo, K., and Nakashima, T. (2000) Methamphetamine-induced striatal dopamine neurotoxicity and cyclooxygenase-2 protein expression in BALB/c mice. *Neuropharmacology 39*, 399–406.

44. Marnett, L. J., and DuBois, R. N. (2002) COX-2: a target for colon cancer prevention. *Annu. Rev. Pharmacol. Toxicol. 42*, 55–80.

45. Oka, A., and Takashima, S. (1997) Induction of cyclooxygenase 2 in brains of patients with Down's syndrome and dementia of Alzheimer type: specific localization in affected neurones and axons. *NeuroReport 8*, 1161–1164.

46. Bernheimer, H., Birkmayer, W., Hornykiewicz, O., Jellinger, K., and Seitelberger, F. (1973) Brain dopamine and the syndromes of Parkinson and Huntington. Clinical, morphological and neurochemical correlations. *J. Neurol. Sci. 20*, 415–455.

47. Compton, J., van Amelsvoort, T., and Murphy, D. (2002) Mood, cognition and Alzheimer's disease. *Best Pract. Res. Clin. Obstet. Gynaecol. 16*, 357–370.

48. Twelves, D., Perkins, K. S., and Counsell, C. (2003) Systematic review of incidence studies of Parkinson's disease. *Mov. Disord. 18*, 19–31.

49. Cadet, J. L., Ladenheim, B., Baum, I., Carlson, E., and Epstein, C. (1994) CuZn-superoxide dismutase (CuZnSOD) transgenic mice show resistance to the lethal effects of methylenedioxyamphetamine (MDA) and of methylenedioxymethamphetamine (MDMA). *Brain Res. 655*, 259–262.

50. Fukumura, M., Cappon, G. D., Broening, H. W., and Vorhees, C. V. (1998) Methamphetamine-induced dopamine and serotonin reductions in neostriatum are not gender specific in rats with comparable hyperthermic responses. *Neurotoxicol. Teratol. 20*, 441–448.

51. Liechti, M. E., Gamma, A., and Vollenweider, F. X. (2001) Gender differences in the subjective effects of MDMA. *Psychopharmacology* (*Berlin*) *154*, 161–168.

52. Dluzen, D. E., and McDermott, J. L. (2002) Estrogen, anti-estrogen, and gender: differences in methamphetamine neurotoxicity. *Ann. N.Y. Acad. Sci. 965*, 136–156.

53. Colado, M. I., Camarero, J., Mechan, A. O., Sanchez, V., Esteban, B., Elliott, J. M., and Green, A. R. (2001) A study of the mechanisms involved in the neurotoxic action of 3,4-methylenedioxymethamphetamine (MDMA, 'ecstasy') on dopamine neurones in mouse brain. *Br. J. Pharmacol. 134*, 1711–1723.

54. Darvesh, A. S., and Gudelsky, G. A. (2004) The relationship between hyperthermia and glycogenolysis in 3,4-methylenedioxymethamphetamine-induced serotonin depletion in rats. *Neurotoxicol. Teratol. 26*, 571–577.

55. O'Shea, E., Esteban, B., Camarero, J., Green, A. R., and Colado, M. I. (2001) Effect of GBR 12909 and fluoxetine on the acute and long term changes induced by MDMA ('ecstasy') on the 5-HT and dopamine concentrations in mouse brain. *Neuropharmacology 40*, 65–74.

DOI: 10.1021/cn900022w | *ACS Chem. Neurosci.* (2010), *1*, 366–380

56. Yeh, S. Y. (1999) N-tert-butyl-alpha-Phenylnitrone protects against 3,4-methylenedioxymethamphetamine-induced depletion of serotonin in rats. *Synapse 31*, 169–177.

57. Spencer, A. G., Woods, J. W., Arakawa, T., Singer, I. I., and Smith, W. L. (1998) Subcellular localization of prostaglandin endoperoxide H synthases-1 and -2 by immunoelectron microscopy. *J. Biol. Chem. 273*, 9886–9893.

58. Mecocci, P., MacGarvey, U., Kaufman, A. E., Koontz, D., Shoffner, J. M., Wallace, D. C., and Beal, M. F. (1993) Oxidative damage to mitochondrial DNA shows marked age-dependent increases in human brain. *Ann. Neurol. 34*, 609–616.

59. Mecocci, P., MacGarvey, U., and Beal, M. F. (1994) Oxidative damage to mitochondrial DNA is increased in Alzheimer's disease. *Ann. Neurol. 36*, 747–751.

60. Volkow, N. D., Chang, L., Wang, G. J., Fowler, J. S., Franceschi, D., Sedler, M., Gatley, S. J., Miller, E., Hitzemann, R., Ding, Y. S., and Logan, J. (2001) Loss of dopamine transporters in methamphetamine abusers recovers with protracted abstinence. *J. Neurosci. 21*, 9414–9418.

61. Volkow, N. D., Chang, L., Wang, G. J., Fowler, J. S., Leonido-Yee, M., Franceschi, D., Sedler, M. J., Gatley, S. J., Hitzemann, R., Ding, Y. S., Logan, J., Wong, C., and Miller, E. N. (2001) Association of dopamine transporter reduction with psychomotor impairment in methamphetamine abusers. *Am. J. Psychiatry 158*, 377–382.

62. Zakzanis, K. K., and Campbell, Z. (2006) Memory impairment in now abstinent MDMA users and continued users: a longitudinal follow-up. *Neurology 66*, 740–741.

63. Gavett, S. H., Madison, S. L., Chulada, P. C., Scarborough, P. E., Qu, W., Boyle, J. E., Tiano, H. F., Lee, C. A., Langenbach, R., Roggli, V. L., and Zeldin, D. C. (1999) Allergic lung responses are increased in prostaglandin H synthase-deficient mice. *J. Clin. Invest. 104*, 721–732.

64. Liu, L., and Wells, P. G. (1995) DNA oxidation as a potential molecular mechanism mediating drug-induced birth defects: phenytoin and structurally related teratogens initiate the formation of 8-hydroxy-2′-deoxyguanosine in vitro and in vivo in murine maternal hepatic and embryonic tissues. *Free Radical Biol. Med. 19*, 639–648.

65. Winn, L. M., and Wells, P. G. (1997) Evidence for embryonic prostaglandin H synthase-catalyzed bioactivation and reactive oxygen species-mediated oxidation of cellular macromolecules in phenytoin and benzo[a]pyrene teratogenesis. *Free Radical Biol. Med. 22*, 607–621.

66. Markwell, M. A., Haas, S. M., Tolbert, N. E., and Bieber, L. L. (1981) Protein Determination in Membrane and Lipoprotein Samples: Manual and Automated Procedures, in *Methods in Enzymology* (Colonick, S. P., and Kapla, N. O., Eds.) pp 296−303, Academic Press, Inc., New York.

DOI: 10.1021/cn900022w | *ACS Chem. Neurosci.* (2010), *1*, 366–380